


**Please cite the Published Version**

Liu, Yingjuan, Choy, Mun-Kit , Abraham, Sabu, Tenin, Gennadiy, Black, Graeme C and Keavney, Bernard D (2023) Atrial Septal Defect (ASD) associated long non-coding RNA STX18-AS1 maintains time-course of in vitro cardiomyocyte differentiation. *Genes and Diseases*, 10 (4). pp. 1150-1153. ISSN 2352-3042

**DOI:** <https://doi.org/10.1016/j.gendis.2022.07.010>

**Publisher:** Elsevier

**Version:** Published Version

**Downloaded from:** <https://e-space.mmu.ac.uk/632786/>

**Usage rights:**  [Creative Commons: Attribution-Noncommercial-No Derivative Works 4.0](https://creativecommons.org/licenses/by-nc-nd/4.0/)

**Additional Information:** This is an open access article which originally appeared in *Genes and Diseases*, published by Elsevier

**Enquiries:**

If you have questions about this document, contact [openresearch@mmu.ac.uk](mailto:openresearch@mmu.ac.uk). Please include the URL of the record in e-space. If you believe that your, or a third party's rights have been compromised through this document please see our Take Down policy (available from <https://www.mmu.ac.uk/library/using-the-library/policies-and-guidelines>)



## RAPID COMMUNICATION

# Atrial Septal Defect (ASD) associated long non-coding RNA *STX18-AS1* maintains time-course of *in vitro* cardiomyocyte differentiation



Congenital heart disease (CHD) is the commonest birth defect, affecting approximately 9.4/1 000 live births.<sup>1</sup> Atrial Septal Defect (ASD) is one of the commonest CHD clinical phenotypes, which frequently requires treatment either in childhood or adulthood, and can lead to severe complications such as right heart failure and cardiac arrhythmia. Previous genome-wide association studies (GWAS) have identified a region of chromosome 4p16 (Ch4p16) associated with the risk of ASD. The most strongly associated SNPs (rs870142, rs6824295 and rs16835979) lie within a 38.8-kb region of linkage disequilibrium encompassing only the long noncoding RNA *STX18-AS1* (also named *LOC100507266*) (Fig. 1A; Fig. S1a). Associated SNPs are expression quantitative trait locus (eQTLs) for *STX18-AS1* in adult ventricular myocardial tissue.<sup>2</sup>

We first confirmed this eQTL association in human atrial tissues and showed it was specific to the myocardium (Fig. S1b–f). GTEx data (<https://gtexportal.org/>) confirmed that the risk SNPs are not eQTLs of any other genes in this region, including *MSX1* and *STX18*, in cardiac tissues. *STX18-AS1*, a lowly conserved lncRNA gene without homologues in mouse (Fig. S2) and the only gene interacting with the linkage disequilibrium (LD) block containing the risk SNPs in the GeneHancer regulatory elements database (Fig. 1A), is therefore the strongest regional candidate gene for the ASD association signal.

Based on the most validated transcript ENST00000610009.5 (mapped to GRCh28. p13), we showed the transcription of *STX18-AS1* is highly stage-dependent during heart development. Compared to adult tissues, *STX18-AS1* was enriched in foetal tissues, including heart, brain, kidney, liver and lung (Fig. S3a). In developing

human hearts, the peak expression of *STX18-AS1* was identified at Carnegie stage (CS) 14–18 (Fig. 1B), overlapping with the critical period for atrial septation.<sup>3</sup> To show the spatial distribution of *STX18-AS1* in developing hearts, we conducted whole mount *in situ* hybridisation with an *STX18-AS1* probe on three whole embryonic hearts at CS17–19. In all three hearts, *STX18-AS1* expression was detected in AS, outflow tract (OFT), atrioventricular cushion (AVC), and part of the ventricles (Fig. S3b–g). The signals are mainly detected in the developing septum and valves/cushions (Fig. S3h–m). In the single CS15 heart available for RNA extraction, the relative quantity of *STX18-AS1* transcripts was found to be higher in the AS than all other segments (Fig. 1C). Thus, levels of *STX18-AS1* transcription accompanied Atrial Septal development spatio-temporally in human hearts.

We next investigated *STX18-AS1* function in human embryonic stem cell differentiated cardiomyocytes (hESC-CM). Based on the H9 human embryonic stem cell line, we created a clonal *STX18-AS1* knockout (KO) line with CRISPR/cas9, targeting the first two exons of *STX18-AS1* with paired sgRNAs by removing ~3.3 kb sequence to stop *STX18-AS1* transcription (Fig. 1D). Transcription of the neighboring gene *STX18* (one rare transcript of which partially overlaps with *STX18-AS1*'s first exon) was confirmed to be unaffected by the CRISPR design (Fig. S4a). We observed a ~30% reduction in transcription of another neighboring gene *MSX1* in KO cells (Fig. S4b); since *MSX1* acts as a “roadblock” to hESC-CM formation, and its deficiency promotes hESC-CM differentiation,<sup>4</sup> this would not explain the delayed hESC-CM differentiation from *STX18-AS1* KO cells we outline below. Moreover, regards relevance to ASD, loss-of-function mutations in *MSX1* in humans cause deficient tooth development without any heart phenotype.<sup>5</sup>

Peer review under responsibility of Chongqing Medical University.

<https://doi.org/10.1016/j.gendis.2022.07.010>

2352-3042/© 2022 The Authors. Publishing services by Elsevier B.V. on behalf of KeAi Communications Co., Ltd. This is an open access article under the CC BY-NC-ND license (<http://creativecommons.org/licenses/by-nc-nd/4.0/>).

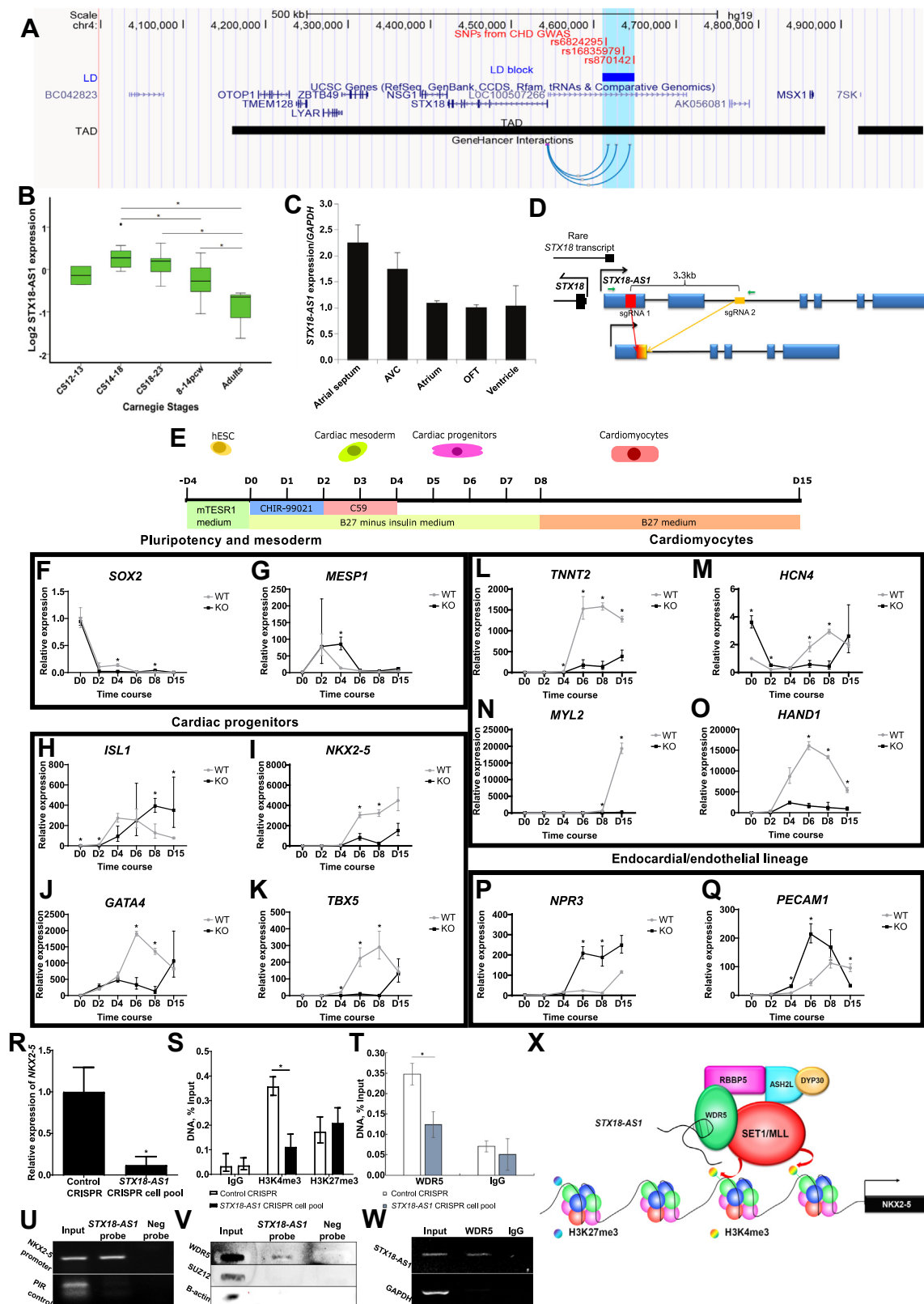


**Figure 1** Long non-coding RNA *STX18-AS1* regulates *in vitro* cardiomyocyte differentiation via epigenetic regulation. (A) The relative genomic location of ASD-risk SNPs and *STX18-AS1* (*LOC100507266*) with surrounding genes and chromosome interactions. GWAS identified top risk SNPs for ASD were labeled as red lines with SNP IDs. The linkage disequilibrium block (LD block in blue rectangle spans 38.8 kb) was extracted from the LD map generated with HaploView using data from 1000 Genomes Project (CEU population). Topologically associating domains (TADs) were aligned with data from 3D genome browser; while the GeneHancer Interaction (available as UCSC genome browser track) only shows the regulatory elements within the LD block region using the data

The *STX18-AS1* CRISPR transduction did not change the morphology, proliferation, apoptosis or pluripotency of undifferentiated H9 cells (Fig. S5). Following a monolayer hESC-CM differentiation protocol (Fig. 1E), *STX18-AS1* KO cells (Fig. S6) produced no beating colony until Day 10, while control wildtype (WT) cells produced abundant beating CMs at Day 6–8 (Videos S1–3). Throughout differentiation to Day 15, *STX18-AS1* KO cells formed beating CM islands of variable sizes and beating rates separated by non-beating cell populations, while the WT CMs formed networks and beat synchronously (Videos S4–5). Cardiomyocytes differentiated from *STX18-AS1* deficient hESC cells were less in Cardiac Troponin T positive rate and weak in Cardiac Troponin T signal (Fig. S7).

Supplementary video related to this article can be found at <https://doi.org/10.1016/j.gendis.2022.07.010>

Time-course data of *STX18-AS1* KO hESC-CM differentiation showed an extended peaking time of *MESP1* (Day 2–4), delayed activation, and reduced transcription of cardiac progenitor markers (*NKX2-5*, *TBX5*, and *GATA4*), a pan-cardiomyocyte marker (*TNNT2*), and both ventricular (*MYL2* and *HAND1*) and atrial (*HCN4*) CM lineage markers at Day 8–15 (Fig. 1F, G and I–O). The increase of *ISL1* in KO cells was slower, and prolonged to Day 15, compared to the peak at Day 6 in WT (Fig. 1H). These results suggest that *STX18-AS1* KO does not entirely stop the programming of cardiomyocyte differentiation *in vitro* but prolonged the duration of cardiac progenitor specification and delayed their differentiation into cardiomyocytes. In support of this notion, endocardial/endothelial lineages (*NPR3* and *PECAM1*) increased during the deferred period of forming cardiac progenitors and early cardiomyocytes (Fig. 1P, Q), suggesting potential endocardial/endothelial lineage substitution for CMs during hESC-CM differentiation from *STX18-AS1* KO cells.

We next investigated the mechanism of downregulation of the known ASD gene *NKX2-5* by *STX18-AS1* KO. We

detected a 70% reduction of H3K4me3 around *NKX2-5*, commensurate with the reduced *NKX2-5* expression (Fig. 1R, S; Fig. S8a–c), in an *STX18-AS1* CRISPR cell pool of HepG2 cells, a cell line chosen owing to its reliably detectable expression of both *STX18-AS1* and *NKX2-5*. In keeping with the reduction of H3K4me3 at *NKX2-5*, the binding affinity of WDR5, a scaffold protein of the SET1/MLL complex required for the trimethylation of H3K4, as reduced by 50% at the promoter region of *NKX2-5* in the *STX18-AS1* CRISPR cell pool (Fig. 1T). Using Chromatin isolation by RNA purification (ChIRP) (Fig. S8d–f), *STX18-AS1* transcripts were shown to interact both with the promoter sequences of *NKX2-5*, and with WDR5 (Fig. 1U, V). RNA immunoprecipitation with WDR5 antibody pulled down detectable *STX18-AS1* RNA (Fig. 1W), confirming the direct interaction between *STX18-AS1* and WDR5 protein. Co-localization of the *STX18-AS1* lncRNA and WDR5 protein at the *NKX2-5* promoter region suggested a direct epigenetic regulative role of *STX18-AS1* on *NKX2-5* (Fig. 1X) and potentially other downstream targeted cardiac transcriptional factors.

In summary, we present multiple lines of evidence suggesting that *STX18-AS1*, a lncRNA at chromosome 4p16, is responsible for the GWAS association with ASD observed in the region. *STX18-AS1* has properties consistent with being a critical regulator of multiple core cardiac transcriptional factors promoting cardiac lineage specification, which merit further characterization. As yet, relatively few CHD GWAS studies have been published; these findings demonstrate the feasibility of gene identification and underscore the potential value of larger studies.

## Conflict of interests

Authors declare no conflict of interests.

from Fishilevich's paper showing the interactions between GeneHancer regulatory elements and genes. (B) Dynamic changes in *STX18-AS1* transcription during human heart development. \*,  $P < 0.05$ . 3–5 samples are included for each developmental period of Carnegie Stages (CS). (C) *STX18-AS1* transcription in different human heart segments (one sample from CS15). (D) The design of the CRISPR sgRNA pair with the cuts at the first exon and second intron of *STX18-AS1*. The sgRNAs do not overlap any transcript of *STX18*. The red rectangle and yellow rectangle represent sgRNA1 and sgRNA2. The gradient colored rectangle indicates the repaired join of two cuts. (E) Time schedule and treatments applied in cardiomyocyte differentiation protocol up to Day 15, and the relevant period of cell stages from hESC to cardiomyocytes. (F, G) The time courses of markers of cell pluripotency (F, *SOX2*) and cardiac mesoderm (G, *MESP1*). (H–K) Markers for cardiac progenitors: *ISL1* (H), pan-cardiac progenitor marker; *NKX2-5* (I), *GATA4* (J), and *TBX5* (K), markers for cardiac progenitors and early cardiomyocytes. (L–O) Time courses of markers for cardiomyocytes: *TNNT2* (L), pan-cardiomyocyte marker; *HCN4* (M), specific marker of atrial cardiomyocytes; *MYL2* (N), marker for ventricular cardiomyocytes; *HAND1* (O), marker for cardiac mesoderm and ventricular cardiomyocytes. (P, Q) Markers of other lineages: *NPR3* (P), marker for endocardial lineage; *PECAM1* (Q), marker for endothelial lineage. Data are shown as Mean  $\pm$  S.E. \*,  $P < 0.05$ . Two-way ANOVA test with Bonferroni adjustment is applied for generating the  $P$  values at each time point ( $n = 3–9$ ). (R) *NKX2-5* transcription level was reduced in *STX18-AS1* CRISPR cell pool of HepG2. (S, T) Using ChIP, H3K4me3 (S) and WDR5 (T) around the promoter of *NKX2-5* was reduced in *STX18-AS1* CRISPR cell pool, without changes in H3K27me3. IgG was used as a background control. (U, V) ChIRP-PCR detected the promoter region of *NKX2-5* in *STX18-AS1* antisense probe pulldown lysate, localizing *STX18-AS1* at the *NKX2-5* promoter (U). The *STX18-AS1* ChIRP probes pulled down WDR5 protein but not SUZ12 and B-actin (background control) detecting with slot blotting (V). A PIR region with rare RNA binding opportunity was used as the background control. (W) RNA immunoprecipitation with anti-WDR5 pulled down *STX18-AS1* RNA transcripts, detected with PCR. IgG was used as negative control antibody. (X) The model of *STX18-AS1*'s trans-activating effects on *NKX2-5* by interacting with SET1/MLL complex and regulating the histone methylation around the downstream target. Data are shown as Mean  $\pm$  S.E. \*,  $P < 0.05$ , comparing to Control CRISPR using T-test or Two-way ANOVA ( $n = 3$ ).

## Funding

This work was supported by The University of Manchester-Peking University Health Science Centre Alliance, the China Scholarships Council, and British Heart Foundation Programme Grant RG/15/12/31616. BK holds a British Heart Foundation Personal Chair. Human embryonic/foetal materials were provided by the Joint MRC/Wellcome Trust (grant#MR/R006237/1) Human Developmental Biology Resource (<http://hdb.org>).

## Acknowledgements

We thank Dr Ruairidh Martin for collection of the samples for eQTL analyses and the data in peripheral blood.

## Appendix A. Supplementary data

Supplementary data to this article can be found online at <https://doi.org/10.1016/j.jgendis.2022.07.010>.

## References

1. Liu Y, Chen S, Zühlke L, et al. Global birth prevalence of congenital heart defects 1970-2017: updated systematic review and meta-analysis of 260 studies. *Int J Epidemiol*. 2019;48(2):455–463.
2. Cordell HJ, Bentham J, Topf A, et al. Genome-wide association study of multiple congenital heart disease phenotypes identifies a susceptibility locus for atrial septal defect at chromosome 4p16. *Nat Genet*. 2013;45(7):822–824.
3. Faber JW, Hagoort J, Moorman AFM, Christoffels VM, Jensen B. Quantified growth of the human embryonic heart. *Biol Open*. 2021;10(2):bio057059.
4. Rao J, Pfeiffer MJ, Frank S, et al. Stepwise clearance of repressive roadblocks drives cardiac induction in human ESCs. *Cell Stem Cell*. 2016;18(3):341–353.
5. Khasawneh RR, Kist R, Queen R, et al. Msx1 haploinsufficiency modifies the Pax9-deficient cardiovascular phenotype. *BMC Dev Biol*. 2021;21(1):14.

Yingjuan Liu <sup>a,\*</sup>, Mun-kit Choy <sup>a</sup>, Sabu Abraham <sup>a</sup>,  
Gennadiy Tenin <sup>a</sup>, Graeme C. Black <sup>b,c</sup>, Bernard  
D. Keavney <sup>a,b,\*\*</sup>

<sup>a</sup> Division of Cardiovascular Sciences, University of  
Manchester, Manchester M13 9PL, UK

<sup>b</sup> Manchester University NHS Foundation Trust, Manchester  
Academic Health Science Centre, Manchester M13 9NQ, UK

<sup>c</sup> Division of Evolution & Genomic Sciences, University of  
Manchester, Manchester M13 9WL, UK

\*Corresponding author.

\*\*Corresponding author. Division of Cardiovascular Sci-  
ences, University of Manchester, Manchester, M13 9PL, UK.  
E-mail addresses: [yingjuan.liu@manchester.ac.uk](mailto:yingjuan.liu@manchester.ac.uk) (Y. Liu),  
[bernard.keavney@manchester.ac.uk](mailto:bernard.keavney@manchester.ac.uk) (B.D. Keavney)

15 November 2021

Available online 8 August 2022